Near-Room-Temperature Soft Plasma Pulsed Deposition of SiC$_x$N$_y$ from 1,3,5-tri(isopropyl)cyclotrisilazane

View the article online for updates and enhancements.

Near-Room-Temperature Soft Plasma Pulsed Deposition of SiC_xN_y from 1,3,5-tri(isopropyl)cyclotrisilazane

Jonathan D. Goff [a], Chad Brick [a], Barry Arkles [a,c], and Alain E. Kaloyeros [b]

[a] Gelest Inc., 11 Steel Road East, Morrisville, PA 19067, USA
[b] BFD Innovation, Slingerlands, New York 12159, USA
[c] Corresponding Author: executiveoffice@gelest.com

Results are presented from an exploratory study of near-room-temperature pulsed deposition of SiC_xN_y thin films using 1,3,5-tri(isopropyl)cyclotrisilazane (TICZ, $C_9H_{27}N_3Si_3$) and soft remote ammonia (NH_3) plasma co-reactants. The process involved four pulses: thermal adsorption of TICZ to the substrate at very low temperature, nitrogen (N_2) purge, soft NH_3 remote plasma step, and N_2 purge. These steps were repeated until the desired film thickness was reached. The ratio of C to N in the films was modulated by controlling the substrate temperature in the range of 30 to 200 °C. In-situ analysis of the deposition process was carried-out using spectroscopic ellipsometry, and the films were analyzed by x-ray photoelectron spectroscopy (XPS). The findings of this study indicate that the combination of reduced substrate thermal budget and soft remote plasma provides an optimum low energy environment for the controlled deposition of SiC_xN_y protective coatings on thermally fragile, chemically sensitive substrates, including plastics and polymers.

Introduction

The silicon carbo-nitride (SiC_xN_y) material system has recently re-emerged as a promising candidate for a plethora of important traditional and new technological applications.[1–3] Its appeal is due not only to its beneficial chemical, physical, electrical, mechanical, and optoelectronic properties,[4] but also to the fact that it can be made to transition from a SiC_x-like to SiN_x-like performance depending on the carbon to nitrogen (C/N) ratio and corresponding chemical bonding configurations.[5]

Among its traditional usages, SiC_xN_y is employed as an inert protective coating and encapsulation layer for systems operating under harsh chemical and thermal environments due to its elevated hardness ($\geq$ 40 GPa), high thermal shock and radiation resistance, efficient oxidation protection, and good thermal and tribological performance.[1,6–8]

SiC_xN_y has also been incorporated into a number of current and emerging applications in copper (Cu)-based multilevel metallization schemes in for integrated circuitry (IC) devices.[9] For example, it is being used as a diffusion barrier against Cu migration into the surrounding low dielectric constant (κ) materials.[7,10] SiC_xN_y is also under consideration as a capping layer and etch stop for copper interconnects, either individually or in combination with selective cobalt capping.[11] Additionally, it is currently

being explored as a dielectric film for inclusion in metal-oxide-nitride-oxide-silicon (MONOS)-type non-volatile memory devices.[12,13]

Furthermore, SiC_xN_y is a leading contender for incorporation into applications requiring adjustable properties, such as tunable optical gap and refractive index. The interest in SiC_xN_y is driven by the fact that its performance can be tightly modulated by adjusting the C and N concentrations. The potential resulting usages include ultraviolet (UV) detectors, "all-silicon" tandem solar cells, flexible electroluminescent displays, and photoluminescence devices.[14–17]

Other SiC_xN_y thin film usages of significant interest include: as active sensing layers in chemical and gas pressure sensors,[18] as well as polymer-derived amorphous SiC_xN_y for integration into high-temperature microelectromechanical systems (MEMS), microsensors, new energy storage devices, and lithium-ion batteries (LIBs).[19,20]

In terms of SiC_xN_y growth processes, most of the reports in the literature have focused on the use of direct current (dc) magnetron sputtering and plasma-enhanced chemical vapor deposition (PE-CVD) at substrate temperatures typically in the range of 350 to 450 °C.[7,12,18] Films were also formed at lower temperatures in a very few cases, but required subsequent annealing at 400 to 450 °C.[7] Other deposition techniques included: (i) electron cyclotron resonance PE-CVD (ECR PE-CVD) at substrate temperatures in the range of 120 to 170°C, followed by annealing between 400 and 1200 °C to enable photoluminescence behavior;[14] (ii) laser-plasma CVD at substrate temperatures of 350 to 850 °C;[6] and (iii) polymer pyrolysis within the substrate temperature range of 1000 to 1600 °C.[19] Efforts to achieve film growth at lower temperatures included inductively-coupled, radio-frequency (RF), PE-CVD at substrate temperatures from 50 to 450 °C using direct argon (Ar) plasma at powers of 100 to 500 W.[21]

However, the use of elevated thermal budget, direct plasma activation, and high plasma power density prevent the deposition of SiC_xN_y on thermally fragile and chemically sensitive substrates, including plastics and polymers. Concerns include thermal, electrical, and mechanical damage to the chemical and compositional integrity and physical structure of such substrates. These concerns are further compounded by the well-documented drive across many industries towards more complex and smaller IC and hetero-device structures, an evolution necessitating the migration from sputtering and traditional PE-CVD towards processing technologies that can deposit ultrathin SiC_xN_y layers conformally in aggressive device topographies, such as atomic layer deposition (ALD) and pulsed CVD (P-CVD).[22]

To address these challenges, work by the present investigators has focused on the implementing of a three-pronged strategy that enables near-room-temperature deposition of SiC_xN_y thin films within a low energy environment. The strategy combines the use of soft remote plasma with P-CVD of N-alkyl substituted perhydridocyclotrisilazanes and a new class of Si source precursors in a reduced thermal budget mode. Contrary to traditional perhydridocyclic silazanes with methyl groups on the N atoms, perhydridocyclotrisilazanes encompass alkyl radicals with at least two carbon atoms on each N atom.[23] The resulting chemical structure offers a pathway for low temperature SiC_xN_y deposition through the controlled and gradual elimination of alkyl groups, and subsequent atomic re-arrangement within the growing SiC_xN_y film.[24,25]

Accordingly, this report describes key results from an exploratory study of near-room-temperature pulsed deposition of SiC_xN_y thin films using one such perhydridocyclo-trisilazane, namely, 1,3,5-tri(isopropyl)cyclotrisilazane (TICZ, $C_9H_{27}N_3Si_3$) and soft remote ammonia (NH_3) plasma as co-reactants. *In situ*, real-time, spectroscopic ellipsometry and x-ray photoelectron spectroscopy (XPS) were used to analyze pertinent SiC_xN_y compositional, physical, and chemical properties, with an emphasis on C/N ratios and bonding configurations. The findings of this study are presented and discussed below.
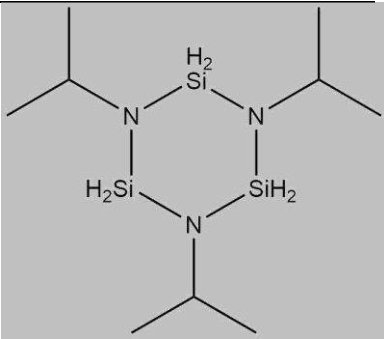
Experimental Conditions

Experimental Deposition Conditions

All experiments were performed in a Picosun R-200 R&D reactor capable of processing substrates up to an 8" sized wafer. The reactor is outfitted with a load-lock system that sequesters sample transport and handling from the reaction chamber, thus ensuring uninterrupted vacuum integrity and effective isolation of the reaction chamber from atmospheric contamination. Plasma is provided remotely through an inductively-coupled plasma (ICP) power generator. In this exploratory study, SiC_xN_y depositions were carried out on 1000 nm-thick silicon dioxide thermally grown on n-doped Si wafers, purchased from Addison Engineering. The substrates were introduced into the reactor without any ex-situ cleaning and were exposed to a pre-deposition remote NH_3 plasma treatment at a plasma frequency of 13.56 MHz and a plasma power of 2000 W for five minutes prior to the actual P-CVD step.

The TICZ Si source precursor is a moisture-sensitive liquid at room temperature, with molecular weight of 261.59 g, melting point of -71 to -69 °C, boiling point of ~220 to 224 °C at 760 torr, and vapor pressure of ~ 1 torr at 70 °C. TICZ was loaded into a dedicated Picosun bubbler in a glovebox under nitrogen (N_2) atmosphere and inserted into the Picosun delivery manifold system, which was heated to ~90 °C to prevent precursor re-condensation before reaching the reaction zone. The bubbler was kept at 50 °C. N_2 was employed as carrier gas and set at a 100 sccm flow rate.

The SiC_xN_y film growth experiments were conducted in two stages. In a first screening stage, systematic scoping experiments were performed to establish optimized P-CVD run parameters, including process working pressure, remote NH_3 plasma power, and precursor, NH_3, and N_2 flow rates, as well as the length of the pre-deposition plasma treatment step, and the duration of the TICZ, N_2 purge, and remote NH_3 plasma pulse steps. Once this stage was completed, and appropriate experimental parameter sets were identified, a second process optimization stage was implemented to determine SiC_xN_y compositional, physical, and chemical properties as a function of substrate temperature in the range of 30 °C to 200 °C. For this stage, the NH_3 flow rate was kept constant at 40 sccm, while remote plasma power and frequency were set at 2000 W and 13.56 MHz, respectively. Table I summarizes the key P-CVD run parameters.

TABLE I. Key Processing Parameters for Soft Remote Plasma SiC_xN_y Deposition.

Processing Parameter	Value	Description
Precursor	TICZ ($C_9H_{27}N_3Si_3$) @50°C	
Substrate Temperature	30-200 °C	30, 50, 60, 90, 120,150, 170, 200
TICZ Pulse Duration	0.4 s	(N_2 carrier gas @100 sccm)
N_2 Purge	2.0 s	@100 sccm
NH_3 Remote Plasma Pulse	10.0 s	@40 sccm, 2000W
N_2 Purge	3.0 s	@100 sccm
ZnO_x Capping Layer	Standard ALD Process Diethyl Zinc (DEZ) and H_2O (10-15 nm thick)	0.1s DEZ pulse, 5 s N_2 purge, 0.1s H_2O pulse, 5 s N_2 purge.

The SiC_xN_y growth runs were followed in-situ with the deposition of an approximately 10 to 15 nm-thick zinc oxide (ZnO_x) capping layer to prevent SiC_xN_y contamination upon exposure to air and during subsequent transport and handling. For the ZnO_x step, a standard ALD process was employed. The substrate temperature was maintained at the same value as the SiC_xN_y deposition step, except in the case of the 50 °C SiC_xN_y film, for which the temperature was increased to 150 °C for the ZnO_x growth step. The ALD ZnO_x process employed the reaction of diethyl zinc (DEZ) and water (H_2O) as the Zn and O sources, respectively: it involved a 0.1 s DEZ pulse and 0.1 s H_2O vapor pulse, separated by 5 s N_2 purge each.

At the conclusion of each deposition run, the samples were transferred back into the load lock system and kept under a N_2 atmosphere until they cooled down to room temperature prior to removal from the Picosun system.

Analytical Techniques

To study the composition and chemical bonding characteristics of the SiC_xN_y films, x-ray photoelectron spectroscopy (XPS) analyses were carried out on a PHI Quantum 2000 system at Eurofins EAG Materials Science, LLC. The system is equipped with a monochromatic Al K_α X-ray source at a primary energy of 1486.6 eV. Incident X-rays are directed at the sample at a ±23° acceptance angle and reflected at a 45° take-off angle. Quantitative analysis as a function of depth in the films was performed by collecting data sequentially at spots within the films after every material removal step using an Ar^+ ion gun at 2 keV primary energy, 4 mm×2 mm raster, and 3.8 nm/min sputter rate. Elemental high resolution binding energy scans were also acquired at varying film depths for Si, C, N, and O. No scan deconvolution was required since the Si, N, C, and O bindings energies are well distinct from each other. CasaXPS software (Casa Software Ltd.) was used to

process and integrate all data, while montage plots were produced by MultiPak software, made by Ulvac-phi, Inc. Profile graphs of composition as a function of film depth in the films were generated using Microcal Origin (Microcal Software, Inc.); the calibration procedure outlined in ISO 15472:2010 "Surface chemical analysis – X-ray photoelectron spectrometers – Calibration of energy scales" was followed in assigning the elemental high resolution binding energy peaks.

In-situ, real-time evaluations of the adsorption and reaction pathways of the TICZ source precursor and NH_3 remote plasma, as well as the resulting SiC_xN_y film nucleation and growth profiles, were performed using angle-resolved ellipsometry on a Woollam iSE ellipsometer at wavelengths ranging from 400 to 1000 nm. The ellipsometer system was attached to the PicoSun reactor and positioned so as to enable the incident light beam to interrogate the substrate at an angle of 60.8° through a quartz glass window. The reflected light beam was collected by a detector through an opposing quartz window. CompleteEASE software was used to perform all data analyses, with the substrate being simulated as a ~1000-nm thick thermal SiO_2 layer on Si. For calibration purposes, the thickness of the SiO_2 layer was quantified in-situ prior to each growth experiment. The optical constants of the SiC_xN_y films were determined by ex-situ ellipsometry analysis.

The film wet etch behavior was examined using an IC industry standard room temperature solution consisting of 0.5 % hydrofluoric acid (HF) in deionized water.

Results and Discussion

XPS Analysis

Table II presents representative atomic concentration percentages of Si, C, N, and O in films deposited at 50, 150, and 200 °C. The values were determined by quantitative XPS analysis, as shown in Figures 1 and 2 for SiC_xN_y samples deposited at 50 and 150 °C, respectively.

TABLE II. Representative atomic concentrations (in at% rounded to the nearest whole number) within the bulk of SiC_xN_y films grown at various substrate temperatures.

Substrate Temperature (°C)	Depth in Sample (nm)	Si	C	N	O
50	~25	~27	~45	~18	~10
150	~25	~43	~17	~37	~3
200	~25	~48	~0	~48	~5

The oxygen content in the films was ~10 at% at 50 °C substrate temperature and decreased to 3-5 at% at higher temperatures. The presence of this small concentration of O could be due to H_2O reaction with SiC_xN_y during the subsequent *in situ* ALD ZnO_x capping layer step. It could also result from impurities in NH_3 or N_2 and/or the well-known issue of plasma etching of the Al_2O_3 dielectric liners that are employed in ICP plasma sources.[26,27] A gradual decrease in C concentration was also observed at higher substrate

temperaturse, while the N content exhibited a steady increase, as shown in Table II and Figures 1 and 2.
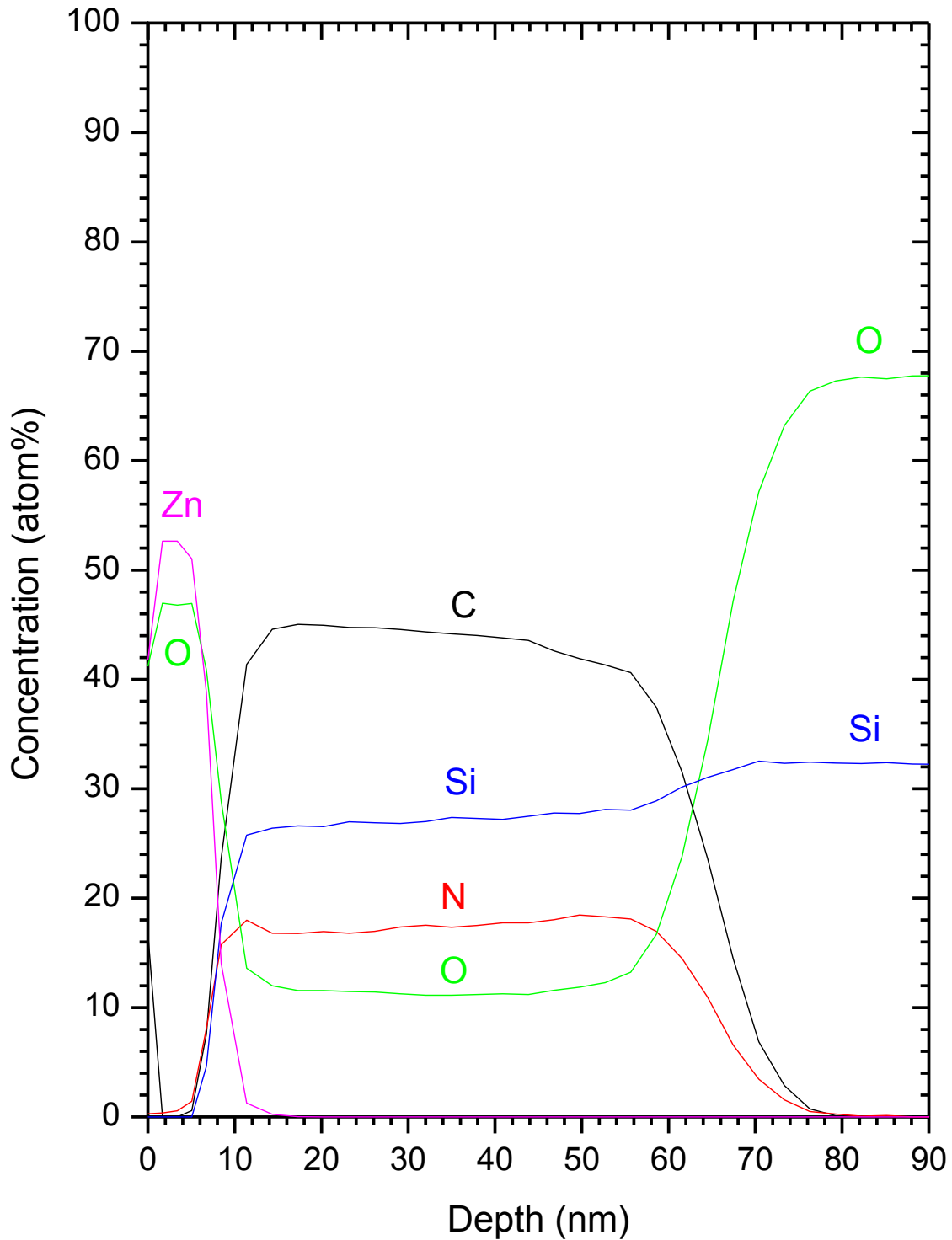

Figure 1. XPS depth profile of Zn, Si, N, C, and O concentrations for SiC_xN_y films deposited at 50 °C.
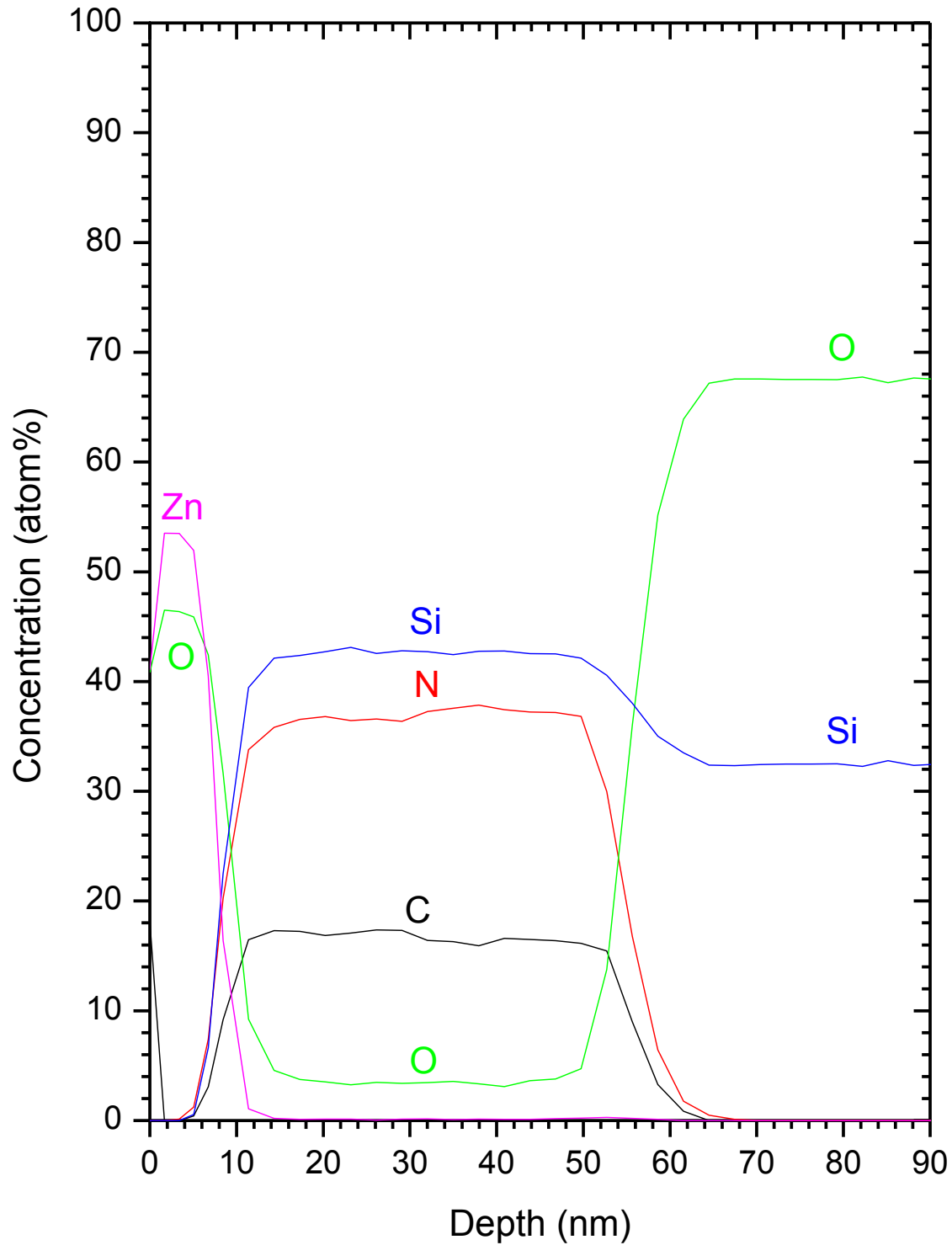
Figure 2. XPS depth profile of Zn, Si, N, C, and O concentrations for SiC_xN_y deposited at 150 ℃.

Figure 3. High-resolution XPS core level spectra for Si2p, N1s, C1s, and O1s binding energies versus penetration depth in SiC$_x$N$_y$ deposited at 50 ^{o}C (film surface located in forefront).
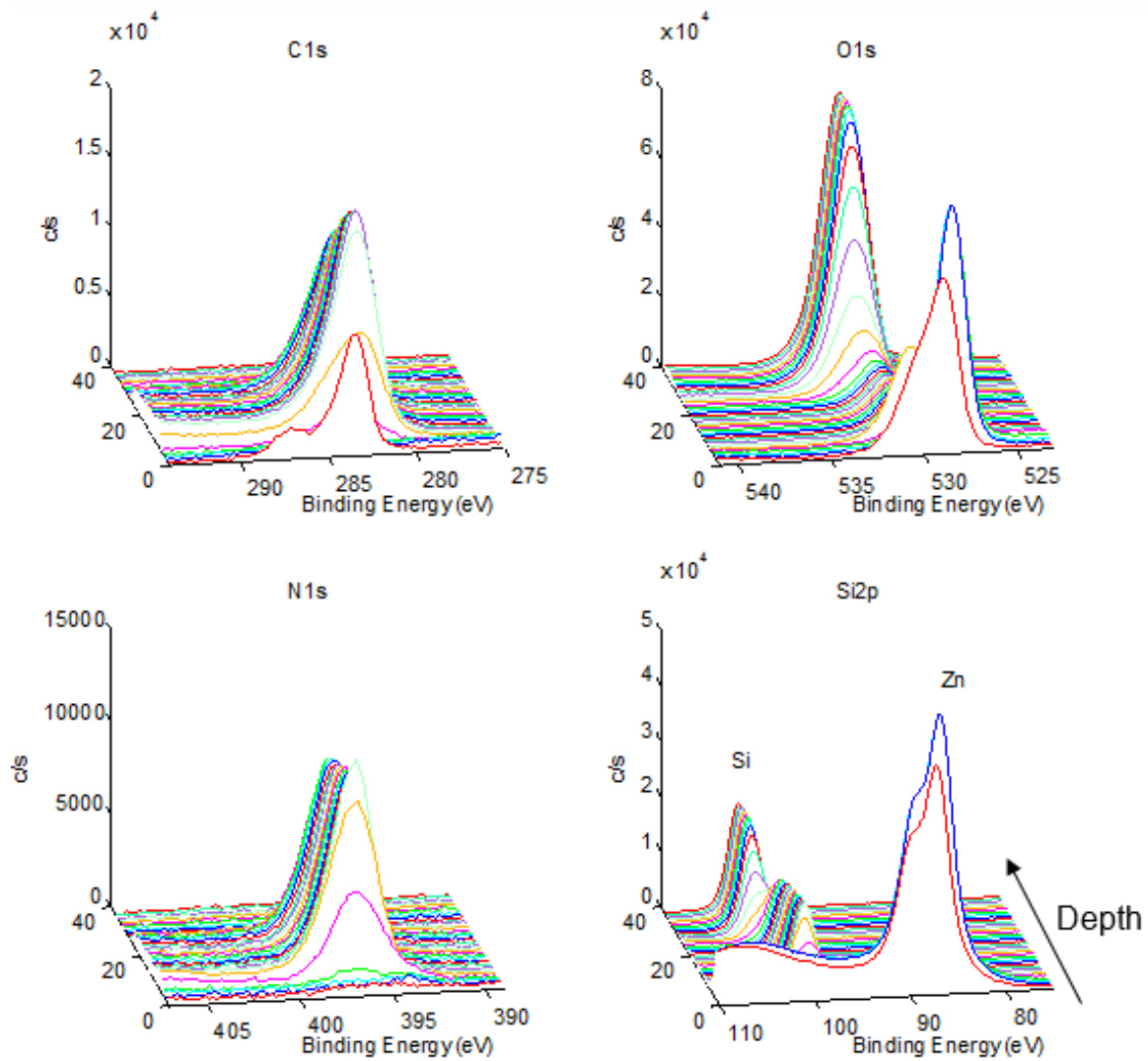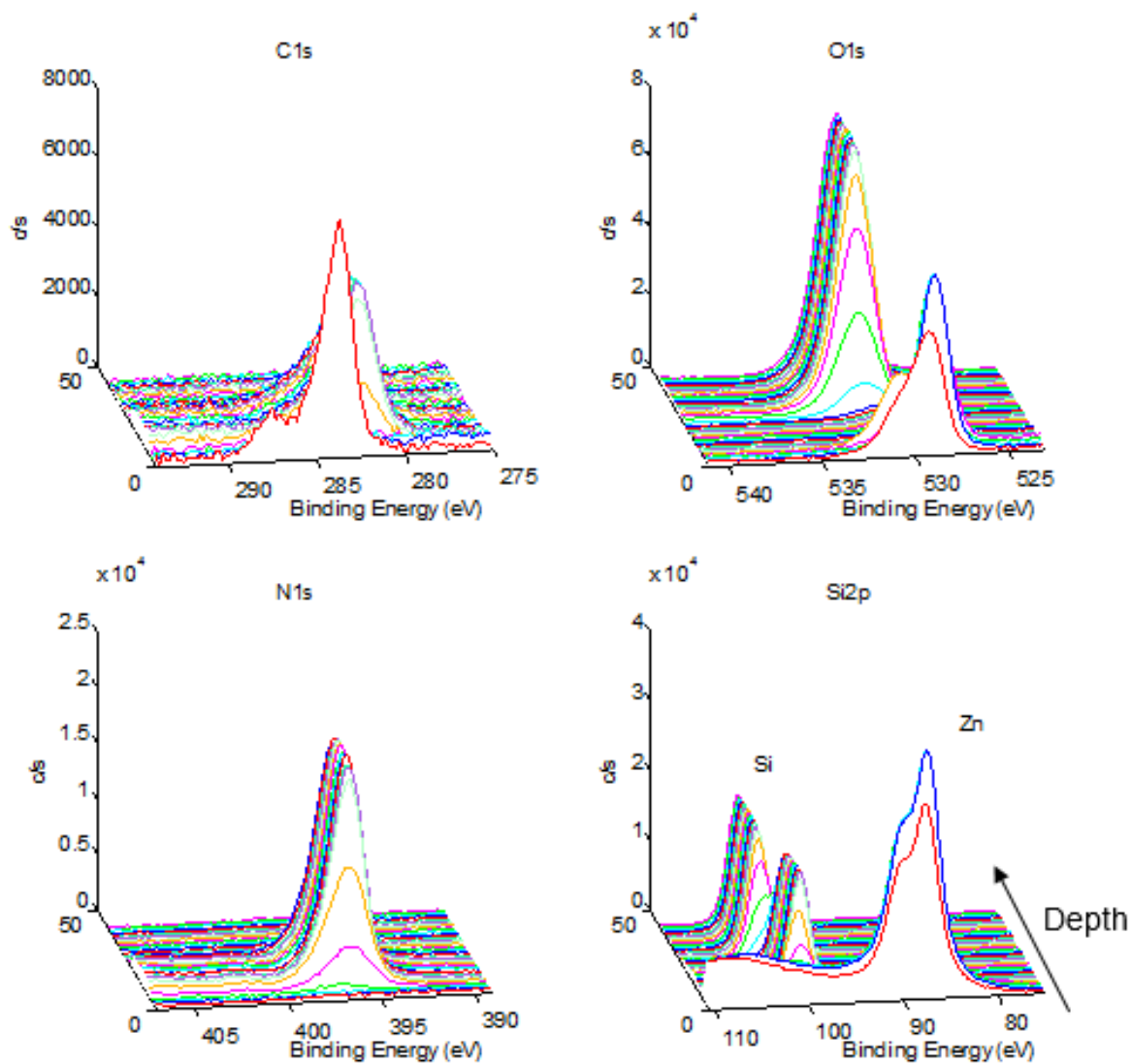
Figure 4. High-resolution XPS core level spectra for Si2p, N1s, C1s, and O1s binding energies versus penetration depth in SiC_xN_y deposited at 150 ºC (film surface located in forefront).

These trends are consistent with the observation that the combination of reduced substrate thermal budget and soft remote plasma provides an optimum low energy environment for the alkyl groups to undergo a gradual and controlled dissociation reaction from the parent molecule; a rise in substrate temperature provides increased thermal activation energy for a higher degree of bond dissociation as well as Si, C, and N bond redistribution within the SiC_xN_y film.

High-resolution XPS core level spectra for Si2p, N1s, C1s, and O1s binding energies versus penetration depth in SiC_xN_y were also compiled for the samples deposited at 50 and 150 °C, respectively, as shown in Figures 3 and 4. Based on the XPS analysis, the location of the Si, N, C, and O core levels peaks appears to be independent of film composition and process thermal budget. More specifically, within the 30 to 150 °C substrate temperature window investigated, the C1s peak location at ~283.3 eV is attributed to C-Si bonds, while the N1s peak position at ~397.3 eV is due to N-Si bonds, regardless of the substrate temperature used. Concurrently, the Si2p peak is composed of contributions from Si-C bonds at ~100.4 eV and Si-N bonds at ~101.7 eV, with perhaps a negligible contribution from Si-O bonds at 103 eV.

The high-resolution XPS analysis seems to indicate that the SiC_xN_y films consist predominantly of a matrix of simple cross-linked Si-C and Si-N bonds for substrate temperatures ≤150 °C. No C is observed in the films within XPS detection limits at 200 °C, with the Si2p and N1s peaks corresponding to a SiN phase.

Our results are different from prior findings in the literature, e.g., atmospheric pressure plasma CVD (AP-PECVD) from triethylsilane ($HSiEt_3$, TES) and N_2 as Si, C, and N sources.[28] In the latter, it was reported that the C1s peak indicated an evolution from C-C to C-Si to C-N type bonds, while the N1s peak exhibited a transition from N-C to predominantly N-Si bonding with some contribution from N-C type bonds. Concurrently, the Si2p were reported to evolve from Si-N, Si-O, and Si-C type bonding to mainly Si-Si bonds, along with Si-N and Si-C bonds. These results were attributed to the presence of various temperature-dependent complex bonding configurations in a-SiCN films, as described in a number of other reports by various researchers.[6,29]
.

XPS analysis therefore supports the assertion that applying a soft remote plasma in concert with a reduced substrate thermal budget in a pulsed CVD mode where the N-alkyl substituted perhydridocyclotrisilazane precursor and NH_3 co-reactant are directed to react only on the substrate surface does yield: (i) a SiC_xN_y matrix with a temperature-independent bonding configuration of simple cross-linked Si-C and Si-N bonds; and (ii) a gradual and controlled decrease in C content with increasing substrate temperature.

Ellipsometry Analysis

In-situ, real-time ellipsometry studies were implemented for the adsorption and reaction pathways of the TICZ source precursor and NH_3 remote plasma, as well as the resulting SiC_xN_y film nucleation and growth profiles, in order to determine the nature and characteristics of the pulsed deposition process. To this end, Figure 5 displays the SiC_xN_y film thickness as a function of deposition time for TICZ pulse times of 0.1, 0.2, 0.4, and 0.8 s. Substrate temperature was maintained at 150 °C in all these runs. The data indicates that film thickness exhibits a steady rise with higher TICZ pulse durations and does not reach a plateau at which it ceases to increase, as would have been expected in an ALD process. It should be noted that this trend is observed across the entire substrate temperature window investigated, indicating that the pulsed deposition of SiC_xN_y does occur in a P-CVD rather than an ALD regime. One advantage of the P-CVD mode is the potential partial decomposition of the parent TICZ precursor upon adsorption to the substrate surface and prior to reaction with NH_3, a feature that is conducive to film deposition in a lower thermal budget window.
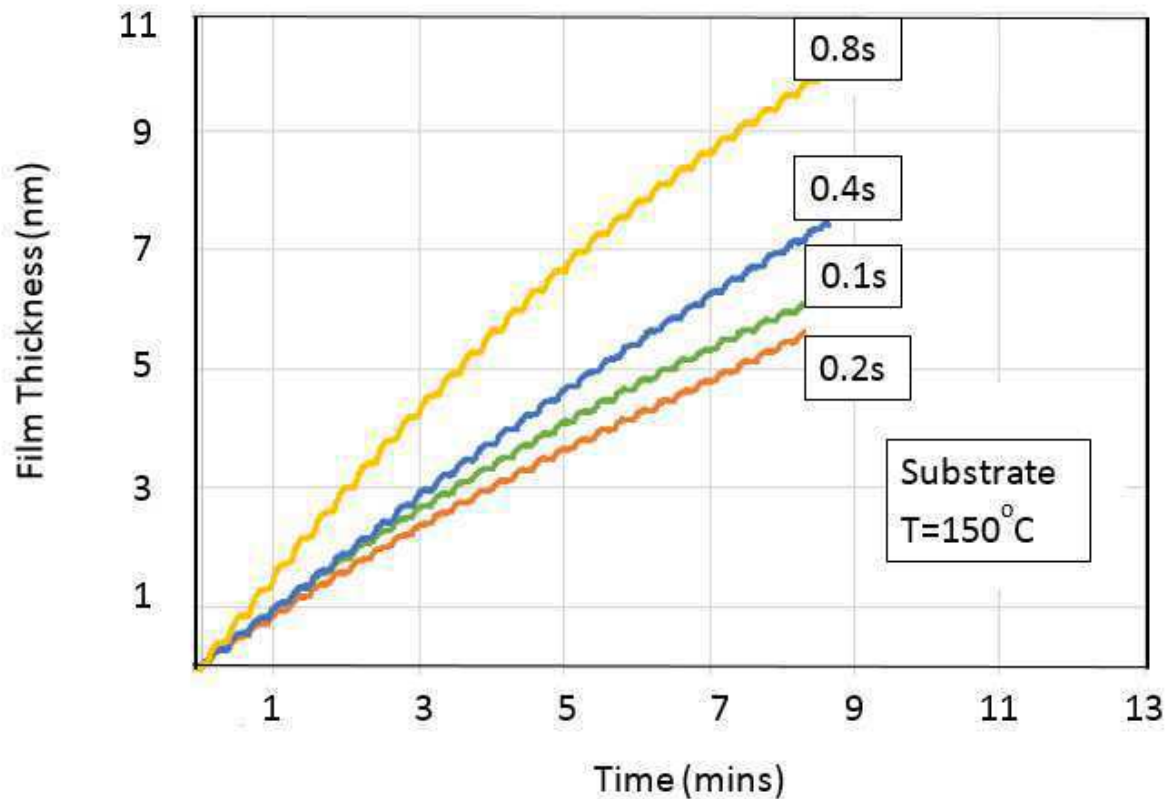
Figure 5. In-situ, real-time, angle-resolved ellipsometry measurements of film thickness versus deposition time for a substrate temperature of 150 ºC and TICZ pulse times of 0.1, 0.2, 0.4, 0.8 s.

Similarly, Figure 6 presents *in situ*, real-time, angle-resolved ellipsometry measurements of film thickness versus deposition time for substrate temperatures of 30, 60, 90, 120, 150, and 170 ºC. The plots show that film nucleation and growth occurs instantaneously, as indicated by the immediate rise in film thickness within the first deposition cycle. This feature is important as it demonstrates the absence of an incubation period prior to the onset of SiC_xN_y film formation, as has been reported in the literature for other ALD and P-CVD work.[3,4,11] The absence of such an incubation period makes P-CVD SiC_xN_y more attractive from a manufacturing perspective by eliminating *ex situ* or *in situ* pre-deposition substrate surface treatments, thereby resulting in a reduction in the number of process steps required to grow SiC_xN_y thin films.
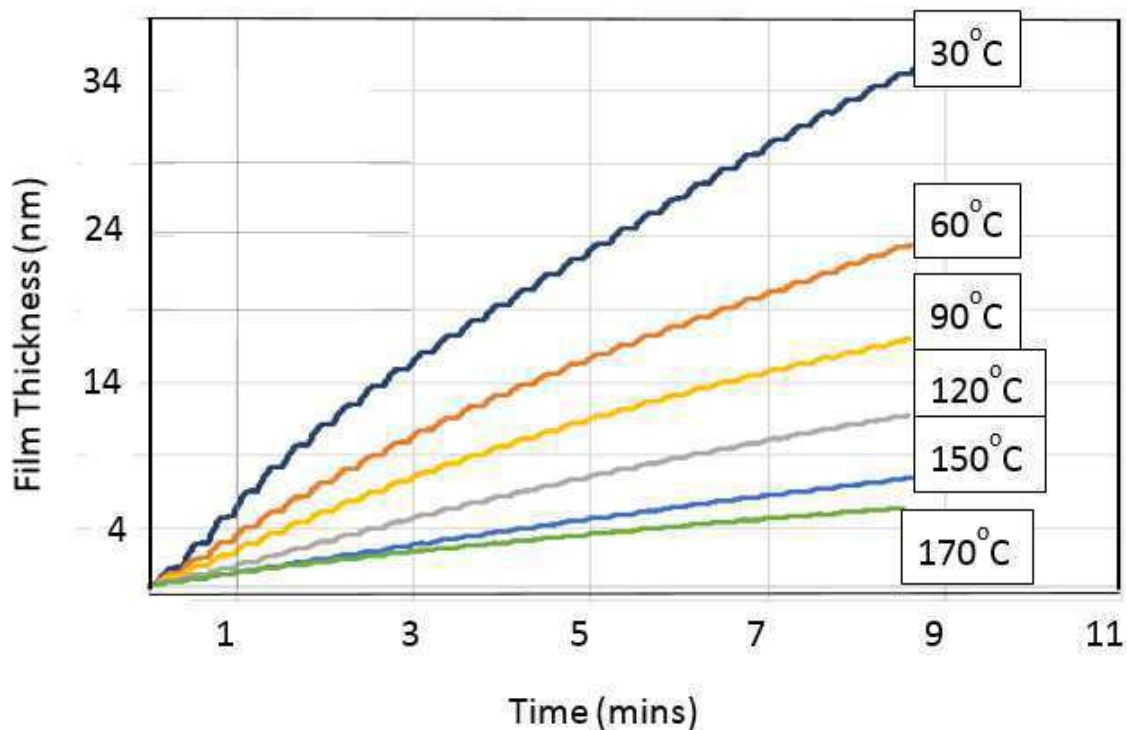
Figure 6. In-situ, real-time, angle-resolved ellipsometry measurements of film thickness versus deposition time for substrate temperatures of 30, 60, 90, 120, 150, and 170 ºC.

Additionally, Figure 6 shows a gradual decrease in the slope of the film thickness curves, and thus the SiC_xN_y growth rate per cycle, with increasing substrate temperature. The reduction in GPC at higher substrate temperatures could potentially be caused by: (i) a decrease in TICZ partial vapor pressure in proximity to the substrate due to the geometry of the reactor, which induces a gradual rise in precursor decomposition at its point of entry into the chamber and prior to reaching the substrate, and/or (ii) a higher rate of desorption of the precursor and associated moieties from the substrate surface prior to the NH_3 co-reactant step due to the rise in thermal budget.

Finally, ex-situ ellipsometry measurements yielded refractive indeces of 1.49, 1.51, and 1.80 for the films deposited at 50, 150, and 200 ºC, respectively.

Wet Etch Rates

Wet etch rate (WER) studies produced values of 2310, 732, and 99 nm/min for the films grown at 50, 150, and 200 ºC, respectively.

Conclusions

An exploratory study of near-room-temperature SiC_xN_y deposition using TICZ and soft remote ammonia (NH_3) plasma as co-reactants yielded SiC_xN_y thin films with $0.40<x<1.67$ and $0.67<y<0.86$ in the substrate temperature range of 30 to 150 ºC. XPS analysis indicated that the SiC_xN_y films consisted predominantly of a temperature-

independent matrix of simple cross-linked Si-C and Si-N bonds. *In situ*, real-time, angle-resolved ellipsometry showed that all films were grown in a P-CVD regime, with film nucleation and growth occurring instantaneously without an incubation period similar to that reported in the literature for other ALD and P-CVD work. This feature makes P-CVD SiC$_x$N$_y$ attractive from a manufacturing perspective due to the elimination of ex-situ or *in situ* pre-deposition substrate surface treatments, leading to an increase in process efficiency and a reduction in both process steps and cost of ownership. Our findings therefore demonstrate that applying a soft remote plasma in concert with a reduced substrate thermal budget in a pulsed CVD mode where TICZ and NH$_3$ co-reactants are directed to react only on the substrate surface constitutes a promising approach for growing of SiC$_x$N$_y$ protective coatings within a low energy environment for potential applications that require thermally fragile, chemically sensitive substrates, including plastics and polymers.

Acknowledgment

References

(1)   Zhuang, C.; Fuchs, R.; Schlemper, C.; Staedler, T.; Jiang, X. Mechanical Behavior of Hard Amorphous Si-C-N Thin Films. *Thin Solid Films* **2015**, *592*, 167–174. https://doi.org/10.1016/j.tsf.2015.09.021.

(2)   Khatami, Z.; Wilson, P. R. J.; Wojcik, J.; Mascher, P. The Influence of Carbon on the Structure and Photoluminescence of Amorphous Silicon Carbonitride Thin Films. *Thin Solid Films* **2017**, *622*, 1–10. https://doi.org/10.1016/j.tsf.2016.12.014.

(3)   Kaloyeros, A. E.; Jové, F. A.; Goff, J.; Arkles, B. Silicon Nitride and Silicon Nitride-Rich Thin Film Technologies: Trends in Deposition Techniques and Related Applications. *ECS J. Solid State Sci. Technol.* **2017**, *6* (10), 691–714. https://doi.org/10.1149/2.0011710jss.

(4)   Kaloyeros, A. E.; Goff, J. D.; Pan, Y.; Arkles, B. Silicon Nitride and Silicon Nitride-Rich Thin Film Technologies: State-of-the-Art Processing Technologies, Properties, and Applications. *ECS J. Solid State Sci. Technol.* **2020**, *in print*.

(5)   Bachar, A.; Bousquet, A.; Mehdi, H.; Monier, G.; Robert-Goumet, C.; Thomas, L.; Belmahi, M.; Goullet, A.; Sauvage, T.; Tomasella, E. Composition and Optical Properties Tunability of Hydrogenated Silicon Carbonitride Thin Films Deposited by Reactive Magnetron Sputtering. *Appl. Surf. Sci.* **2018**, *444*, 293–302. https://doi.org/https://doi.org/10.1016/j.apsusc.2018.03.040.

(6)   Demin, V. N.; Smirnova, T. P.; Borisov, V. O.; Grachev, G. N.; Smirnov, A. L.; Khomyakov, M. N. Physical-Chemical Properties of Silicon Carbonitride Films Prepared Using Laser-Plasma Deposition from Hexamethyldisilazane. *Glas. Phys. Chem.* **2015**, *41* (2), 232–236. https://doi.org/10.1134/S1087659615020042.

(7)   Chang, W.-Y.; Chung, H.-T.; Chen, Y.-C.; Leu, J. Broadband UV-Assisted Thermal Annealing of Low-k Silicon Carbonitride Films Using a C-Rich Silazane Precursor. *J. Vac. Sci. Technol. B* **2018**, *36* (6), 60601. https://doi.org/10.1116/1.5063294.

(8)   Fainer, N. I.; Kosyakov, V. I. Phase Composition of Thin Silicon Carbonitride Films Obtained by Plazma Endanced Chemical Vapour Deposition Using Organosilicon

Compounds. *J. Struct. Chem.* **2015**, *56* (1), 163–174.
https://doi.org/10.1134/S0022476615010229.

(9)   King, S. W. Dielectric Barrier, Etch Stop, and Metal Capping Materials for State of the Art and beyond Metal Interconnects. *ECS J. Solid State Sci. Technol.* **2015**, *4* (1), N3029–N3047. https://doi.org/10.1149/2.0051501jss.

(10)   Mutch, M. J.; Lenahan, P. M.; King, S. W. Spin Transport, Magnetoresistance, and Electrically Detected Magnetic Resonance in Amorphous Hydrogenated Silicon Nitride. *Appl. Phys. Lett.* **2016**, *109* (6). https://doi.org/10.1063/1.4960810.

(11)   Kaloyeros, A. E.; Pan, Y.; Goff, J.; Arkles, B. Cobalt Thin Films: Trends in Processing Technologies and Emerging Applications. *ECS J. Solid State Sci. Technol.* **2019**, *8* (2), P119--P152. https://doi.org/10.1149/2.0051902jss.

(12)   Al Ahmed, S. R.; Kobayashi, K. Extraction of Energy Distribution of Electrons Trapped in Silicon Carbonitride (SiCN) Charge Trapping Films. *IEICE Trans. Electron.* **2017**, *E100C* (7), 662–668. https://doi.org/10.1587/transele.E100.C.662.

(13)   Kobayashi, K.; Mino, H. Hole Trapping Capability of Silicon Carbonitride Charge Trap Layers. *Eur. Phys. J. Appl. Phys.* **2020**.
https://doi.org/10.1051/epjap/2020190297.

(14)   Khatami, Z.; Wilson, P. R. J.; Wojcik, J.; Mascher, P. On the Origin of White Light Emission from Nanostructured Silicon Carbonitride Thin Films. *J. Lumin.* **2018**, *196*, 504–510. https://doi.org/10.1016/j.jlumin.2017.12.011.

(15)   Khatami, Z.; Bosco, G. B. F.; Wojcik, J.; Tessler, L. R.; Mascher, P. Influence of Deposition Conditions on the Characteristics of Luminescent Silicon Carbonitride Thin Films. *ECS J. Solid State Sci. Technol.* **2018**, *7* (2), N7–N14. https://doi.org/10.1149/2.0151802jss.

(16)   Fainer, N. I.; Nemkova, A. A. Optical Properties of Silicon Carbonitride Films Produced by Plasma-Induced Decomposition of Organic Silicon Compounds. *High Energy Chem.* **2015**, *49* (4), 273–281. https://doi.org/10.1134/S0018143915040074.

(17)   Lee, J. S.; Sahu, B. B.; Han, J. G. Simple Realization of Efficient Barrier Performance of a Single Layer Silicon Nitride Film via Plasma Chemistry. *Phys. Chem. Chem. Phys.* **2016**, *18* (47), 32198–32209.
https://doi.org/10.1039/c6cp06722k.

(18)   Kozak, A. O.; Porada, O. K.; Ivashchenko, V. I.; Ivashchenko, L. A.; Scrynskyy, P. L.; Tomila, T. V.; Manzhara, V. S. Comparative Investigation of Si-C-N Films Prepared by Plasma Enhanced Chemical Vapour Deposition and Magnetron Sputtering. *Appl. Surf. Sci.* **2017**, *425*, 646–653.
https://doi.org/10.1016/j.apsusc.2017.06.332.

(19)   Feng, Y.; Dou, S.; Wei, Y.; Zhang, Y.; Song, X.; Li, X.; Battaglia, V. S. Preparation and Capacity-Fading Investigation of Polymer-Derived Silicon Carbonitride Anode for Lithium-Ion Battery. *ACS Omega* **2017**, *2* (11), 8075–8085.
https://doi.org/10.1021/acsomega.7b01462.

(20)   Ma, B.; Wang, Y.; Chen, Y.; Gao, Y. Dielectric Property and Interfacial Polarization of Polymer-Derived Amorphous Silicon Carbonitride. *Ceram. Int.* **2017**, *43* (15), 12209–12212. https://doi.org/10.1016/j.ceramint.2017.06.081.

(21)   Rumyantsev, Y. M.; Chagin, M. N.; Kosinova, M. L.; Kuznetsov, F. A. Synthesis of Thin Silicon Carbonitride Films from Hexamethyldisilazane in an Inductively Coupled Plasma Reactor. *Inorg. Mater.* **2015**, *51* (9), 897–902.
https://doi.org/10.1134/S0020168515090162.

(22)   Kaloyeros, A. E.; Goff, J. D.; Arkles, B. Emerging Molecular and Atomic Level Techniques for Nanoscale Applications. *Electrochem. Soc. Interface* **2018**, *27* (4),

59–63.

(23)   Arkles, B.; Brick, C.; Goff, J. D.; Kaloyeros, A. E. The Low-Temperature Remote-Plasma-Activated Pulsed CVD Route to SiN_x from 1,3,5-tri(isopropyl)cyclotri-silazane. *Thin Solid Films* **2020**, *711, 138299,* doi.org/10.1016/j.tsf.2020.138299.

(24)   Arkles, B.; Pan, Y.; Jove, F. N-Alkyl Substituted Cyclic and Oligomeric Perhydridosilazanes and Silicon Nitride Films Formed Therefrom. *EP 3,274,354 B1* **2019**.

(25)   Arkles, B. Silicon Nitride from Organosilazane Cyclic and Linear Prepolymers. *ECS J. Accel. Br. Commun.* **1986**, *133* (1), 232–234.

(26)   Shih, H.-Y.; Lin, M.-C.; Chen, L.-Y.; Chen, M.-J. Uniform {GaN} Thin Films Grown on (100) Silicon by Remote Plasma Atomic Layer Deposition. *Nanotechnology* **2014**, *26* (1), 14002. https://doi.org/10.1088/0957-4484/26/1/014002.

(27)   Motamedi, P.; Cadien, K. Structural and Optical Characterization of Low-Temperature ALD Crystalline AlN. *J. Cryst. Growth* **2015**, *421*, 45–52. https://doi.org/https://doi.org/10.1016/j.jcrysgro.2015.04.009.

(28)   Guruvenket, S.; Andrie, S.; Simon, M.; Johnson, K. W.; Sailer, R. A. Atmospheric Pressure Plasma CVD of Amorphous Hydrogenated Silicon Carbonitride (a-SiCN:H) Films Using Triethylsilane and Nitrogen. *Plasma Process. Polym.* **2011**, *8* (12), 1126–1136. https://doi.org/10.1002/ppap.201100035.

(29)   Awad, Y.; El Khakani, M. A.; Scarlete, M.; Aktik, C.; Smirani, R.; Camiré, N.; Lessard, M.; Mouine, J. Structural Analysis of Silicon Carbon Nitride Films Prepared by Vapor Transport-Chemical Vapor Deposition. *J. Appl. Phys.* **2010**, *107* (3), 33517. https://doi.org/10.1063/1.3289732.